

PCCP

Accepted Manuscript



This is an *Accepted Manuscript*, which has been through the Royal Society of Chemistry peer review process and has been accepted for publication.

Accepted Manuscripts are published online shortly after acceptance, before technical editing, formatting and proof reading. Using this free service, authors can make their results available to the community, in citable form, before we publish the edited article. We will replace this *Accepted Manuscript* with the edited and formatted *Advance Article* as soon as it is available.

You can find more information about *Accepted Manuscripts* in the [Information for Authors](#).

Please note that technical editing may introduce minor changes to the text and/or graphics, which may alter content. The journal's standard [Terms & Conditions](#) and the [Ethical guidelines](#) still apply. In no event shall the Royal Society of Chemistry be held responsible for any errors or omissions in this *Accepted Manuscript* or any consequences arising from the use of any information it contains.

Cite this: DOI: 10.1039/c0xx00000x

www.rsc.org/xxxxxx

ARTICLE TYPE

Diffusive and Non-diffusive Photo-induced Proton Coupled Electron Transfer from hydrogen bonded phenols to meso-tetrakis-5,10,15,20-Pentafluorophenyl Porphyrin[†]

P. Hemant Kumar, Y. Venkatesh, S. Prashanthi, D. Siva, B. Ramakrishna and Prakriti Ranjan Bangal*

5 Received (in XXX, XXX) XthXXXXXXXXXX 20XX, Accepted Xth XXXXXXXXXXXX 20XX

DOI: 10.1039/b000000x

Enhanced reductive fluorescence quenching of meso-tetrakis- 5,10,15,20-Pentafluorophenyl Porphyrin (H₂F₂₀TPP) by two different phenols, 4-Methoxy phenol (4-MeOPhOH) and 2,6-Dimethoxy phenol (2,6-DiMeOPhOH) in presence of various pyridine bases in dichloromethane solution is studied by steady state and time resolved fluorescence spectroscopic methods by employing time correlated single photon counting (TCSPC) and fluorescence up-conversion techniques. Enhanced quenching behaviour of H₂F₂₀TPP is observed when phenols are hydrogen bonded to various pyridine bases. Quenching observed in steady state and time resolved studies in nanosecond time domain follows second order kinetics and generates quenching rate constants and hydrogen bonded equilibrium constants, the latter which agree quite closely with those obtained from independent spectroscopic measurements. Significant kinetic deuterium isotope effect is observed indicating the importance of proton movement in the quenching processes. This quenching effect is attributed to be due to a tri-molecular transition state involving H₂F₂₀TPP and hydrogen bonded phenol complex, in which electron transfer from phenol to excited H₂F₂₀TPP is concerted with proton movement from phenol to hydrogen bonded base. Observed quenching behaviours are rationalized by invoking diffusion controlled Proton Coupled electron transfer. Fluorescence Up-Conversion studies in 100 ps time domain confirm the ultrafast PCET for 4-MeOPhOH and bases pairs which falls in non-diffusive regime.

1. Introduction

Electron and proton transfer are the most fundamental and ubiquitous processes in chemistry. Isolated electron¹ and proton² transfer processes has been quite well studied subjects over the decades. However coupled electron and proton transfer phenomenon is gaining importance over the past few years because of its importance in various chemical and biological processes.³ Chemical reactions involving simultaneous transfer of both electrons and protons occur widely in organic, inorganic and other areas of chemistry. These coupled electron and proton transfer reactions can occur in a step wise or concerted manner. Step wise mechanism may involve initial electron transfer followed by proton transfer (ET-PT) or proton transfer followed by electron transfer (PT-ET). However processes in which electron and proton transfer occur in a concerted way are termed as Proton Coupled Electron Transfer (PCET)⁴ and it has been defined as a single chemical reaction step involving concerted movement of electron and proton from donor to acceptor. The

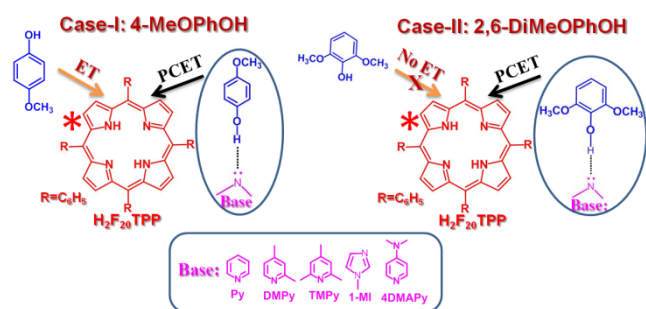
concerted mechanism is highly favoured because it bypasses the formation of high energy intermediates and electrostatic charge buildups.⁵ Depending on the extent and phasing of the proton displacement in PCET it may correspond to a wide range of processes⁶⁻¹⁰ including hydrogen atom transfer (HAT).¹¹ In non-HAT processes where e^- and H^+ are separated leading to the formation of an anion radical, a deprotonated reductant and a protonated base whereas in HAT, e^- and H^+ are transferred together as hydrogen atom. HAT is a well-recognised mechanism of organic free radical chemistry but PCET is relatively less well understood. This PCET phenomenon is being studied recently both experimentally and theoretically by many groups, however most of the study is done through electrochemistry³⁻⁵ and photo-physical aspects of PCET reaction are sparse¹²⁻¹³ in view of literature available on electrochemical studies.

Porphyrins are an important class of macro-cyclic systems found in many biological and chemical systems. They play an important role in diverse fields of research such as catalysis, solar energy conversion, in development of advanced functional materials and in primary process of photosynthesis.¹⁴⁻¹⁸ Their electronic absorption and emission properties are strongly influenced by their peripheral and central substitutions. In earlier reports pertaining to the general problem of coupled electron proton transfer in porphyrin based system, we have given

Inorganic and Physical Chemistry Division, CSIR- Indian Institute of Chemical Technology, Uppal Road, Tarnaka, 500007 Hyderabad, India. E-mail: prakriti@iict.res.in; Fax: (+)90-40-27160921

[†] Electronic Supplementary Information (ESI) available: Additional spectroscopic data. See DOI: 10.1039/b000000x/

evidence for the occurrence of concerted charge movement from various phenols to Pyridyl Porphyrins¹² where quenching of excited singlet state of porphyrin involved bimolecular complex in the transition state, in which electron transfer from phenol to excited porphyrin was coupled with proton movement from phenol to the associated pyridine. In that case porphyrin played a dual role of acting as an electron and proton acceptor and phenol acted as electron and proton donor. We now extend the study further from bimolecular to tri-molecular reaction system involving individual electron acceptor, proton acceptor and electron-proton donor. Meso-tetrakis-Pentafluorophenyl Porphyrin ($H_2F_{20}TPP$), a free base porphyrin in which pentafluorophenyl groups are covalently linked to four meso positions of the porphyrin macro-cycle acts as an excellent electron acceptor. Its reductive quenching behaviour with various aliphatic amines has been studied previously in our group¹⁹ and now we intend to study the system with two different phenols, 4-methoxy phenol (4-MeOPhOH) and 2,6-dimethoxy phenol (2,6-DiMeOPhOH) having nearly similar oxidation potential. In this article we report (Scheme 1), how the photo-induced electron transfer rate from phenols to $H_2F_{20}TPP$ is enhanced by the added pyridine bases (Case-I) and how photo-induced electron transfer is ignited upon addition of bases (Case-II).



Scheme.1 Chemical structure of Porphyrin, Phenols and Bases used in the present study.

2. Experimental

Meso-tetrakis-5,10,15,20-PentafluorophenylPorphyrin ($H_2F_{20}TPP$) purchased from Porphyrin System, Germany and used as received. 4-Methoxy phenol (4-MeOPhOH), 2,6-Dimethoxy phenol (2,6-DiMeOPhOH) and all the pyridines (pyridine(Py), 2,4-Lutidine(DMPy), 1,3,5-Trimethylpyridine(TMPy), 1-Methyl Imidazole(1-MI) and 4-Dimethylamino Pyridine(4DMApy)) were purchased from Aldrich Chemicals, USA and spectroscopic grade dichloromethane(DCM) is purchased from Merck, Germany. Phenols were sublimed and pyridines were distilled before use. Phenols were deuterated by fast exchange with C_2H_5OD ($D > 99\%$), added to the solution in more than 20-fold excess.

All UV/vis spectra were recorded using Hitachi U-2910 spectrophotometer. IR spectral studies were done using Cary Series UV-Vis-NIR spectrophotometer. Spectroscopic titrations were done in DCM solutions of respective phenols by successive addition of various pyridine bases for obtaining hydrogen bond equilibrium constants between phenols and pyridines. Equilibrium constant K_{HB} , for the formation of hydrogen-bond complexes were calculated from the change in absorbance at

given wavelength on added reagent (respective pyridines) using the relation given by Mataga and Tsuno.²⁰

$$(1-d_0/d)/[B] = -K_{HB} + (\epsilon_C/\epsilon)K_{HB} (d_0/d) \quad (1)$$

where K_{HB} is the hydrogen bonding equilibrium constant, ϵ_C and ϵ respectively, denote the extinction coefficient of the complex and free molecule and d_0 , d are absorbance in absence and presence of bonding agent (B is different pyridines) whose total concentration is much higher than that of phenols. The intercept of the plot $(1-d_0/d)/[B]$ Vs $(\epsilon_C/\epsilon)K_{HB} (d_0/d)$ is $-K_{HB}$.

All steady state fluorescence spectra were recorded at room temperature by Fluorolog-3 spectrofluorimeter of Horiba JobinYvon exciting on any of the Q-band where Change of absorbance is less due to added H-bonding agent. Lifetime measurements were done either by TCSPC system (Model-5000U) of Horiba Jobin Yvon, Stanmore, U.K, with 490 nm LED or by a SPC-130 TCSPC module (Becker & Hickl) coupled with our fluorescence up-conversion set up. The normal lifetime (τ_0) of $H_2F_{20}TPP = 9.8$ ns. All quenching (steady state and time resolved) experiments were done in DCM solvent with $\sim 2 \times 10^{-5}$ M concentration of porphyrin. Fluorescence quantum yield (ϕ) is determined using secondary standard method described elsewhere taking Tetraphenyl porphyrin (H_2TPP) as reference ($\phi = 0.13$). The steady state and time resolved spectrophotometric titration process adopted here is very simple and described in brief, solutions (3 mL) in DCM of porphyrin of known concentration (1-5 μ M) and 10mM-20mM of phenols were titrated directly into a 1 cm quartz fluorimeter cell by successive addition of increasingly concentrated pyridine solutions in DCM (0.01-0.5M), from a microliter syringe.

To perform Fluorescence up-conversion study FOG100 system (CDP System) was used. Part of the pulsed (690-1040 nm) Ti:sapphire (Mai Tai HP, Spectra Physics) fundamental laser output (~ 500 mW at 800 nm) was steered into CDP2015 frequency conversion unit to have second (SH) and third harmonic (TH) as desired. A beam splitter (BS) is used to split the input beam to excitation (SH/TH pulses) and gate (fundamental residual pulses) beams. The excitation beam directed to a rotating sample cell with the help of six BSs and one mirror. A lens ($f=40$ mm) was used to focus excitation beam into the sample. A ND filter was used for the excitation attenuation. The gate beam was directed by two mirrors to gold-coated retro-reflector mirror connected to 8 ns optical delay line before being focused together with the fluorescence (collected by an achromatic doublet, $f=80$ mm) on 0.5 mm type I BBO crystal. The angle of the crystal was adjusted to phase matching conditions at the fluorescence wavelength of interest. The upconverted signal (in the UV range) was focused with a lens ($f=60$ mm) to an input slit of the monochromator (CDP 2022D). The intensity of the up-converted radiation was measured with a photomultiplier tube operating in the photon counting mode. Proper filters were used before the detector to eliminate parasitic light from the upconverted signal if any. The polarization of the excitation pulses was set at magic angle relative to that of the gate pulses using Berek's variable wave plate. The sample solutions were placed in a 0.6 mm or 1 mm rotating cell and absorbance of about ~ 1 at excitation wavelength generally used (yielding a concentration around 100-200 μ M). The FWHM of the IRF in

this setup was calculated about 240 fs in the 0.4 mm cell and 280 fs in the 1 mm cell. Hence, a time resolution of around 200 fs could be achieved. This time resolution is mainly limited by the optics and the duration of the laser pulses. For data analysis, the fluorescence time profile at a given emission wavelength $I(\lambda, t)$ was reproduced by the convolution of a Gaussian IRF with a sum of exponential trial function representing the pure sample dynamics $S(t)$. Gaussian term was added to account for fast non-exponential processes if any owing to vibrational or other solvent relaxation process.

3. Results and discussion

3.1 Spectroscopic Hydrogen Bonding Equilibrium Constants

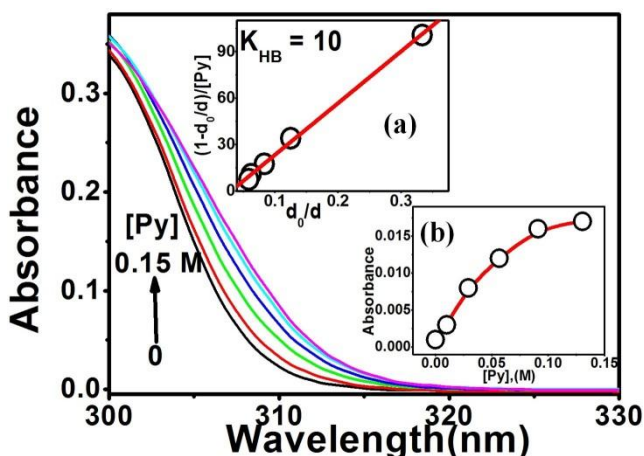


Fig. 1 Change in absorption spectra of 4-MeOPhOH with addition of Py. Inset: (a) shows the Mataga plot at 315nm. (b) Change of absorbance due to formation of 4-MeOPhOH-Py complex as function of Py concentration.

From the very nature of phenols and pyridine base it is obvious that they form hydrogen bonded complex when dissolved in aprotic solvents and the H-bonding equilibrium strongly depend on the polarity of the solvents.^{6a, 26} Here we measure hydrogen bonding equilibrium constant (K_{HB}) between 4-MeOPhOH and different bases in DCM at room temperature by UV-Vis spectrophotometric titration. Fig. 1 illustrates the change of 4-MeOPhOH absorbance upon successive addition of Py. A red shift of long wavelength phenol absorption upon hydrogen bonding is evident and application of eq 1 to these systems yields K_{HB} values presented in Table 1. Same is also determined from the change of OH overtone band of phenol at around 1425 nm, where no interference of absorbance due to added base, as function of different bases concentration and listed in the Table 1 for comparison. It is noteworthy to mention that measured K_{HB} values by two different methods are parallel although values obtained in UV-Vis titration method bit high and it can be due to partial overlap of Py's absorption with that of 4-MeOPhOH. However, UV-Vis spectroscopic determination of the hydrogen bonding equilibrium constants between 2,6-DiMeOPhOH and different bases is apparently difficult due to strong overlap of the absorption spectra of phenol and bases as well as change of absorbance as function of base is too weak to measure. However, the K_{HB} values between 2,6-DiMeOPhOH and different bases are calculated from the change of absorbance of OH overtone band as

a function of different base concentrations. Upon successive addition of pyridines in DCM solution of 2,6-DiMeOPhOH, the absorbance of OH overtone peak at around 1450 nm decreases due to hydrogen bonded complex formation between them.²¹ Linear Mataga and Tsuno plot estimates the K_{HB} values for respective bases in Table 1

3.2 Steady State and time resolved studies

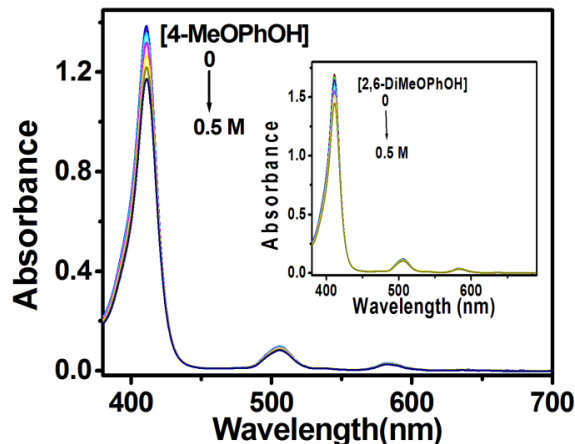


Fig. 2. Change in absorption spectra of $H_2F_{20}TPP$ as a function of 4-MeOPhOH. Inset: Change in absorption spectra of $H_2F_{20}TPP$ as a function of 2,6-DiMeOPhOH.

The steady state spectroscopic properties of $H_2F_{20}TPP$ in DCM solution in terms of electronic absorption and fluorescence spectra has been described elsewhere¹⁹. In brief, it has strong Soret band at 411 nm and two weak Q bands at 505 (Q_y , 0-0) and 580 (Q_x , 0-0) nm. Upon excitation either on Soret band or on Q band it shows fluorescence peaking at 640 nm and 707 nm with fluorescence quantum yield (ϕ_f) \sim 0.06 and natural singlet lifetime (τ_0) \sim 10 ns obtained from TCSPC measurement. The UV/Vis spectroscopic titration of few micro molar solution of $H_2F_{20}TPP$ in DCM by 4-MeOPhOH, 2,6-DiMeOPhOH causes no major change in the whole range of absorption spectra ruling out any possibility of the formation of ground state complex between $H_2F_{20}TPP$ and studied phenols (Fig.2). At very high concentration of phenols slight reduction of Soret band could be observed and it could be due to a very weak interaction of OH group of phenol to the pyrrole-N- atom of porphyrin macro cycle. Similar behaviour is also observed for tetraphenyl porphyrin (H_2TPP) and it does not affect the fluorescence properties of H_2TPP .

However, as shown in Fig. 3, upon addition of 4-MeOPhOH (Case-1) to the solution of $H_2F_{20}TPP$ ($\sim 5 \times 10^{-5}$ M), the fluorescence intensity decreases without any deformation of the fluorescence spectral profile. Similarly, excited singlet lifetime of $H_2F_{20}TPP$ measured by TCSPC method strongly decreases in commensurate to the increased concentration of 4-MeOPhOH (Fig.4) and this decrease of lifetime reveals that this is a dynamic quenching process. Relative fluorescence intensity (I_0/I) and fluorescence lifetime (τ_0/τ) change show exactly similar linear dependence to the 4-MeOPhOH concentration. This linear relationship of the relative fluorescence intensities change (I_0/I) or lifetimes change (τ_0/τ) at any given wavelength follow the Stern-Volmer (S-V) bimolecular kinetic model as below,

$$\frac{I_0}{I} \text{ or } \frac{\tau_0}{\tau} = 1 + K_Q [Q] = 1 + k_Q \tau_0 [Q] \quad (2)$$

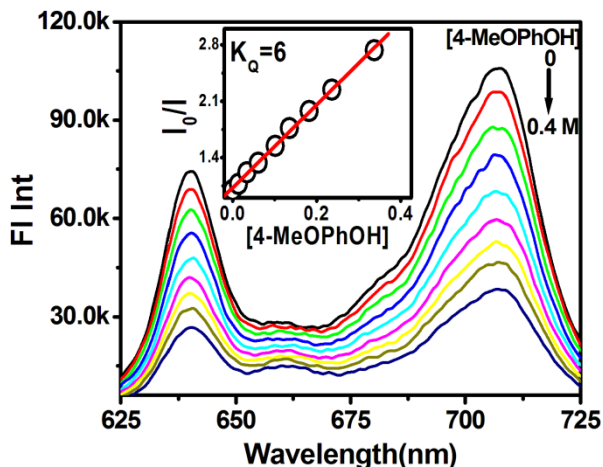


Fig. 3 Change of fluorescence intensity of H₂F₂₀TPP upon successive addition of 4-MeOPhOH, $\lambda_{\text{ex}}=590$ nm.

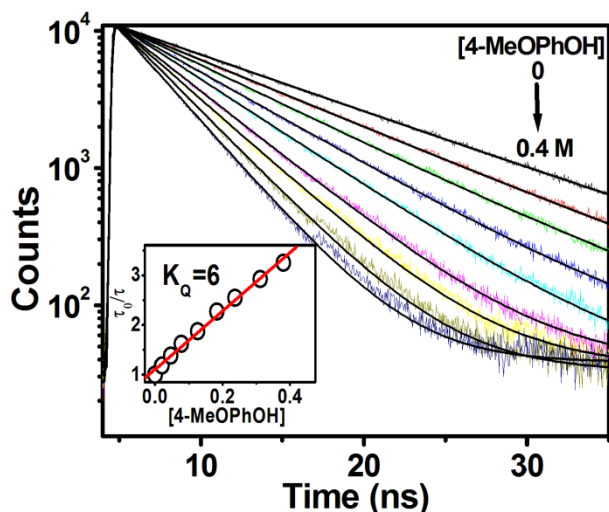


Fig. 4 Change of fluorescence lifetime of H₂F₂₀TPP upon successive addition of 4-MeOPhOH, $\lambda_{\text{ex}}=490$ nm.

where I_0 and I or τ_0 and τ are the relative fluorescence intensities and lifetimes of H₂F₂₀TPP, without and with 4-MeOPhOH concentrations $[Q]$, K_Q is the Stern–Volmer constant, and k_Q is quenching rate constant. From this linear S-V plot K_Q was extracted to be 6 M^{-1} yielding k_Q (K_Q/τ_0) to be $6 \times 10^8 \text{ M}^{-1} \text{ s}^{-1}$. The thermodynamic driving force ΔG_{ET}^0 for electron transfer from 4-MeOPhOH to singlet H₂F₂₀TPP is calculated according to the Rehm–Weller model²² to be exergonic by ~ 0.15 eV, for an oxidation potential, E_{ox} of 4-MeOPhOH (electron donor) of 1.09 V²³ reduction potential, E_{red} of H₂F₂₀TPP (electron acceptor) of 0.7V²⁴ optical excitation energy, ΔE_{00} of H₂F₂₀TPP of 1.94 eV (640 nm) and a Coulomb term assumed to be zero. Hence, this quenching is attributed to be the reduction of excited H₂F₂₀TPP by this phenol. In steady-state conditions the rate of electron transfer from phenol to excited H₂F₂₀TPP can be calculated from the observed bimolecular quenching constant using the standard diffusion controlled mechanism as below,

$$\frac{1}{k_Q} = \frac{1}{k_d} + \frac{1}{K k_{\text{et}}} \quad (3)$$

where K (k_d/k_{et}) is the diffusional equilibrium constant for the

encounter complex formation and can be estimated using Fuoss–Eigen model²⁵. The k_d and K values for present donor-acceptor pair can safely be assumed to be $\sim 1.7 \times 10^{10} \text{ M}^{-1} \text{ s}^{-1}$ and $\sim 2 \text{ mol}^{-1} \text{ dm}^3$ respectively in comparison to the DABCO and H₂F₂₀TPP, donor-acceptor pair¹⁹ and k_{et} is calculated to be $3.1 \times 10^8 \text{ s}^{-1}$. However, in Case-II similar experiment shows negligibly small (S-V constant $K_Q \sim 0.3$, Fig.S3 ESI†) quenching of the fluorescence by 2,6-DiMeOPhOH although it has favourable ΔG_{ET}^0 value. This result indicates that electron transfer from 2,6-DiMeOPhOH is not kinetically favoured process.

The quenching of fluorescence as well as quenching of fluorescence lifetime of H₂F₂₀TPP by 4-MeOPhOH is dramatically enhanced by the addition of different pyridine bases. Fig.5 shows a typical enhanced quenching behavior of excited singlet state of H₂F₂₀TPP as a function of base concentration for a given concentration of 4-MeOPhOH (10 mM). It is important to mention here that, relative change of fluorescence intensity and fluorescence lifetimes are exactly same. The enhancement of this quenching is in parallel to the base strength of added bases ongoing from pyridine (Py) to 4-dimethylamino pyridine (4DMAPy). The relative base strength of the used bases in DCM solvent is assumed to be in the same order as in aqueous solution and corresponding relative pKa values of the bases are listed in the Table 1. Similar titration of H₂F₂₀TPP in presence of different concentrations of 4-MeOPhOH shows proportionate change of fluorescence quenching for same concentration of base (Fig.S1,S2 ESI†). Reverse titration i.e. change of fluorescence intensity or fluorescence lifetime of H₂F₂₀TPP in DCM solution as function of 4-MeOPhOH concentration for a given concentration of base shows similar type of quenching behavior as observed in Fig 5. The S-V plot based on fluorescence intensity change (I_0/I) or lifetime change (τ_0/τ) is convex in nature in all the cases. It is imperative to allude that hydrogen bonded adducts formation follows similar kinds of nonlinearity when base is added to phenol solution (Fig. 1c). Hence, these results clearly indicate that hydrogen bonding equilibrium between phenol and base dictates the nonlinearity of the S-V plot and hydrogen bonded adducts enhanced the quenching of fluorescence of H₂F₂₀TPP. At the same time change of fluorescence lifetime claims that quenching involved in this process is purely dynamic. This typical quenching process can be described by the modified S-V equation as below

$$\frac{I_0}{I} = 1 + K_Q[Q] + K_{\text{QB}}[QB] \quad (4)$$

where K_Q , K_{QB} are assigned as S-V constants for pure and hydrogen bonded phenol-base complex respectively. For the case where total added base $[B]_0 \gg [Q]_0$, eq 4 can modified to eq 5 (see ESI†).

$$\frac{I_0}{I} = 1 + \frac{(K_{\text{QB}} - K_Q) * K_{\text{HB}} * [Q]_0 * [B]_0}{1 + K_{\text{HB}} * [B]_0} \quad (5)$$

where $[Q]_0$, $[B]_0$ are the total concentration of phenol and base respectively and $K_{\text{HB}} (= [QB]/([Q]*[B]))$ is the hydrogen bond equilibrium constant between phenol and base. The enhanced quenching constants (k_{QB}) as well as hydrogen bonding equilibrium constants (K_{HB}) are calculated by NLS fit to the eq (5). The quenching constants found to be in the order of increasing base strength (Table 1) and these are one order below

Cite this: DOI: 10.1039/coxx00000x

www.rsc.org/xxxxxx

ARTICLE TYPE

Table 1: Kinetics in diffusive regime and spectroscopic data of quenching of H₂F₂₀TPP by various phenol-Base systems in DCM solvent.

Phenol	Base	pK _a	E _{ox}	K _{HB} (M ⁻¹)		Kinetic	-ΔG (eV)	K _{QB} (M ⁻¹)	k _{QB} * 10 ⁻⁹ (M ⁻¹ s ⁻¹)	k _{PCET} * 10 ⁻⁹ (s ⁻¹)
				UV-Vis	IR					
4-MeOPhOH	--	--	1.09	--	--	--	0.15	6±1 ^a	0.6±0.1 ^b	0.3±0.1 ^c
	Py	5.22	0.64	10±1	7±2	8±2	0.6	10±1	1±0.1	0.5±0.1
	DMPy	6.99		11±2	8±2	9±2		11±1	1.1±0.1	0.5±0.1
	TMPy	7.43	0.56	14±2	9±2	10±2	0.68	12±1	1.2±0.1	0.6±0.1
	1-MI	6.95		17±3	13±3	13±2		18±1	1.9±0.1	0.8±0.1
4DMAPy	9.70		<i>d</i>	15±3	14±3		50±3	5±0.3	2.5±0.1	
2,6-DiMeOPhOH	--	--	1.06				0.18	--	--	
	Py	5.22	0.48	<i>d</i>	1.5±0.5	1±0.5	0.76	19±2	2±0.2	1±0.2
	DMPy	6.99		<i>d</i>	2±0.5	1±0.5		25±2	2.5±0.2	1.2±0.2
	TMPy	7.43	0.39	<i>d</i>	2±0.5	1±0.5	0.85	26±2	2.7±0.3	1.3±0.3
	1-MI	6.95		<i>d</i>	3±0.5	1±0.5		28±2	2.9±0.3	1.5±0.3
4DMAPy	9.70		<i>d</i>	4±0.5	2±0.5		64±4	6.5±0.5	3.3±0.5	

^aS-V constant in absence of any base, i.e K_Q, ^b quenching rate constant in absence of base (k_Q), ^c electron transfer rate constant (k_{et}), ^d too weak to measure K_{HB} in this method due to complete overlap of phenol and base absorption.

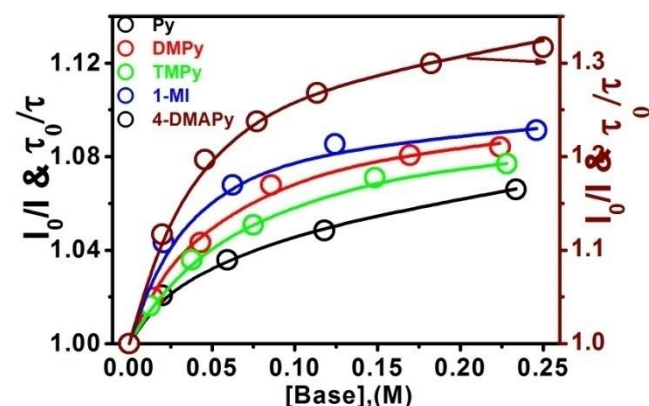


Fig. 5 Enhanced quenching kinetics of H₂F₂₀TPP (20 μM) as a function of different bases in presence of 10 mM 4-MeOPhOH

the diffusion control rate constant (<10⁻¹⁰M⁻¹ s⁻¹). This result reveals that hydrogen bonded phenol-base pair is responsible for this enhanced quenching. Due to the dynamic nature of this quenching we attribute this quenching to be electron transfer from hydrogen bonded phenol-base pair to singlet excited H₂F₂₀TPP. Considering the simple bimolecular diffusion control model of electron transfer and using the eq (3) the rate of electron transfer is calculated and placed in the Table 1.

As for the Case-II, addition of 2,6-DiMeOPhOH shows negligible weak fluorescence quenching of excited state of H₂F₂₀TPP in DCM solution (k_Q → ~10⁶M⁻¹s⁻¹) but addition of pyridine bases causes sharp quenching of fluorescence of H₂F₂₀TPP. Fig 6 shows the quenching behaviour of excited singlet of H₂F₂₀TPP for a given concentration of 2,6-DiMeOPhOH (10 mM) as a function of base concentration. The S-V plots based on fluorescence intensity and lifetime changes are convex in nature for all studied bases. The quenching efficiency increases on increasing the basicity of the used bases. The quenching rate is nicely described by modified S-V equation

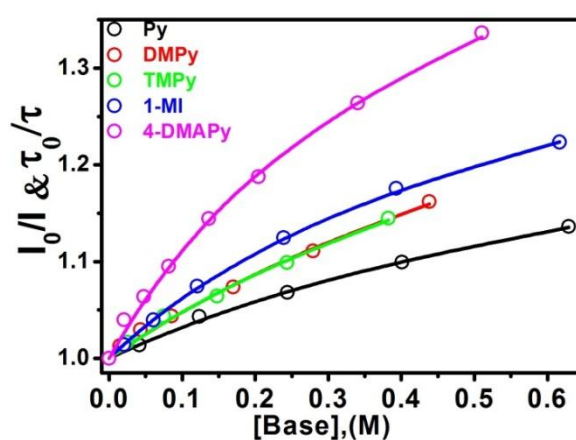


Fig. 6 Enhanced quenching kinetics of H₂F₂₀TPP (20 μM) as a function of different bases in presence of 10 mM 2,6-DiMeOPhOH.

(6),(for more see ESI†)

$$\frac{I_0}{I} = 1 + K_{QB} * \frac{K_{HB} * [Q]_0 * [B]_0}{1 + K_{HB} * [B]_0} \quad (6)$$

Hence, quenching in these cases is mediated by the hydrogen bond phenol-base complexes and these quenching processes are purely dynamic in nature. This attributed quenching rate constant (k_{QB}) and K_{HB} values obtained by NLS fit are listed in Table 1.

The observed quenching rate constants are under diffusion control limit. Likewise case I, we ascribed this quenching process to electron transfer from hydrogen bonded 2,6-DiMeOPhOH-base pair to singlet excited H₂F₂₀TPP. Similarly, the rate of electron transfer is calculated under the diffusion control mechanism and they are listed in Table 1. For the cases of electron transfer studied here are involved with tri-molecular complex and a special diffusion model is required to calculate the exact rate of electron transfer and it is out of the scope of this present study. However, K_{HB} values determined by kinetic

measurements using model eq 5 & eq 6 for 4-MeOPhOH and 2,6-DiMeOPhOH respectively are in reasonably good agreement with those obtained from spectroscopic method. Overall, the K_{HB} values obtained for both the phenols for different bases qualitatively agree with previously observed values for the same systems.^{6a,26} Thus we ascertain with confidence that, hydrogen bonded phenol-base pair reductively quenches $H_2F_{20}TPP$ fluorescence for both the phenol systems. In addition, oxidation potential of phenols bonded to pyridine bases are reduced, which in turn increases the thermodynamic driving force (Table1) for electron transfer reaction to occur ($\Delta G^0_{PCET} > (\Delta G^0_{ET})$).²⁷ Hence, it is apparently clear that in Case-I enhancement of fluorescence quenching of $H_2F_{20}TPP$ in presence of pyridines and appearance of fluorescence quenching of $H_2F_{20}TPP$ in presence of pyridines in Case-II are due to hydrogen bond induced electron transfer reaction.

Deuterium kinetic isotope effect has been done to testify the role of hydrogen bonded proton to the electron transfer reaction for both the cases. In general, for a PCET reaction, deuterium kinetic isotope effect is an essential evidence for the involvement of

deuteration kinetic isotope effects on $k_{QB}(\tau_0/\tau)$ values for the $H_2F_{20}TPP$ and 4DMAPy-4-MeOPhOH system. The dynamic deuteration effect was carried out replacing the OH group of phenol by OD using C_2H_5OD solution and it is found that the reaction rate is substantially lowered by deuteration. The $k_{QB} / {}^Dk_{QB}$ value is significantly greater than 1. This positive isotope effect observed for all cases establishes the clear involvement of concerted proton movement in the electron transfer process and this enhanced quenching process is ascribed to the photo-induced reductive PCET reaction for both the cases. Hence, rate of electron transfer (k_{et}) for both the cases calculated under bimolecular diffusion controlled mechanism is nothing but the rate of proton coupled electron transfer (k_{PCET}).

3.3 Ultrafast Dynamics

In order to explore the time scale of proton movement in this PCET reaction, we have studied the quenching process for these systems in few picoseconds time domain by fluorescence up-conversion technique in 4:1 dichloromethane and tetrahydrofuran solvent mixture. The mechanism of ultrafast relaxation process $H_2F_{20}TPP$ is bit typical and has not been published elsewhere so far and it will be discussed in detail elsewhere very soon. However, in brief, the fluorescence up-conversion signal of $H_2F_{20}TPP$ in 100 ps time domain (Fig.8) by and large follows the pattern as observed for H_2TPP ²⁸ and it is best described by three components fit when excited at Soret band. A 1-2 ps decay (τ_1, a_1), ~ 100 ps rise ($\tau_2, -a_2$) and a very long component of ~ 10 ns decay (τ_3, a_3) which could correspond to the value of excited singlet lifetime of $H_2F_{20}TPP$ observed by TCSPC. In the multi-component fitting process, the decay time of long component was kept fixed where as amplitude was allowed to vary along with all other decay components and their respective amplitudes. The consequence of long component decay time has been tested in the fitting to extract the short component parameters in this 100 ps time domain and it was found that the long component decay does not influence much in the fitting for the estimation of short component parameters. Full characterization of long component decay is done in long time evolution by TCSPC method. Now, in presence of 4-MeOPhOH (up to 0.5M) a bit reduction of rise component could be observed in fluorescence decay profile of $H_2F_{20}TPP$ while no additional decay component could be observed. This reduction of rise component could be due to the interaction of OH group of phenol and pyrrole-N-atom of $H_2F_{20}TPP$ in presence of excessive amount phenol in the solution. However, as shown in Fig 9, upon addition of 4DMAPy very fast component ($\tau_1 \sim 2ps$) does not change but the rise component completely vanishes and an additional fast decay component of 40 ± 10 ps arises (${}^{fast}\tau_{QB}, a_{QB}$) along with slow decay of ~ 1.5 ns which was observed earlier by nanosecond TCSPC measurement. This decay profile is independent to the concentration of 4DMAPy in the range of 0.01M to 0.5 M for given concentration of 4-MeOPhOH. Variation of 4-MeOPhOH concentration does not affect the decay time (40 ± 10 ps) of this component while alter the amplitude of this component. Exactly similar quenching behaviour of fluorescence up-conversion signal is observed for other studied bases and corresponding decay time and amplitude are listed in Table 2. As shown in Table 2, the decay time of the newly appear fast component decreases on increasing basicity of

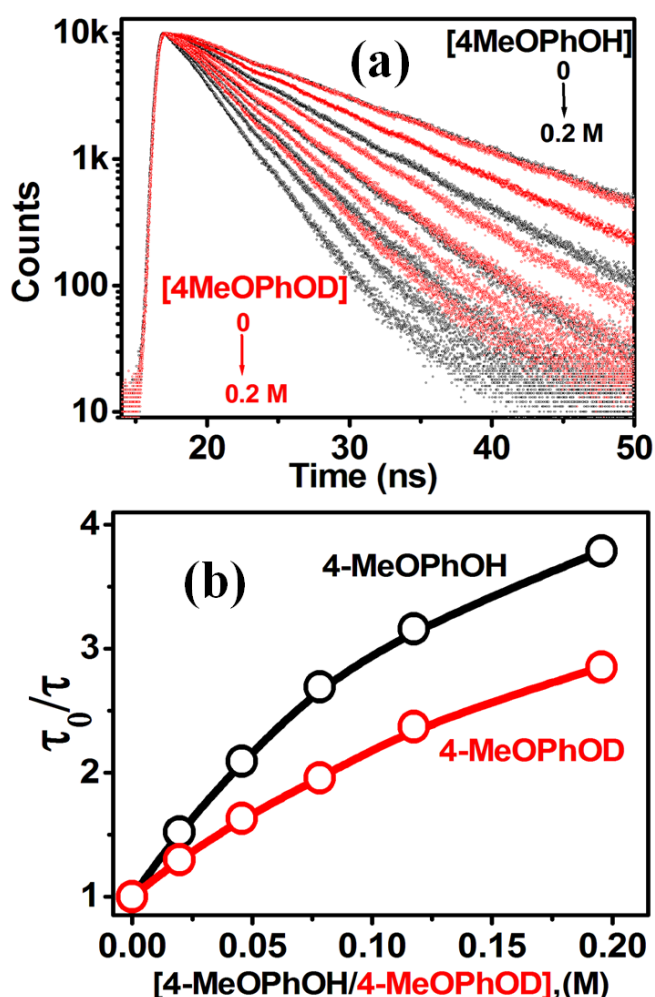


Fig. 7 (a) Change of fluorescence lifetime of $H_2F_{20}TPP$ as a function of 4-MeOPhOH(black)/4-MeOPhOD(red) in presence of 0.1M 4DMAPy, (b) Corresponding S-V plot as a function of added 4-MeOPhOH (black)/4-MeOPhOD(red). $\lambda_{ex}=490$ nm.

phenolic proton in the quenching process.²⁷ Fig.7 shows a typical

Cite this: DOI: 10.1039/coxx00000x

www.rsc.org/xxxxxx

ARTICLE TYPE

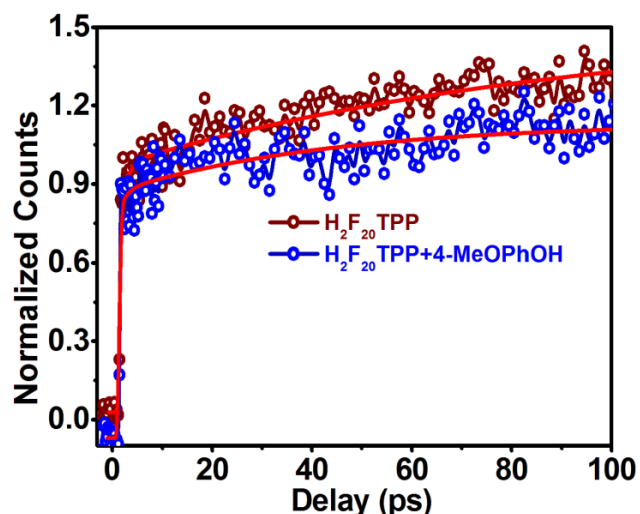


Fig. 8 Fluorescence up-conversion kinetics of $H_2F_{20}TPP$ & $H_2F_{20}TPP + 4-MeOPhOH$ in 4:1 DCM and THF solution, $\lambda_{ex}=410$ nm. Solid red lines are three components exponential fits of the experimental data.

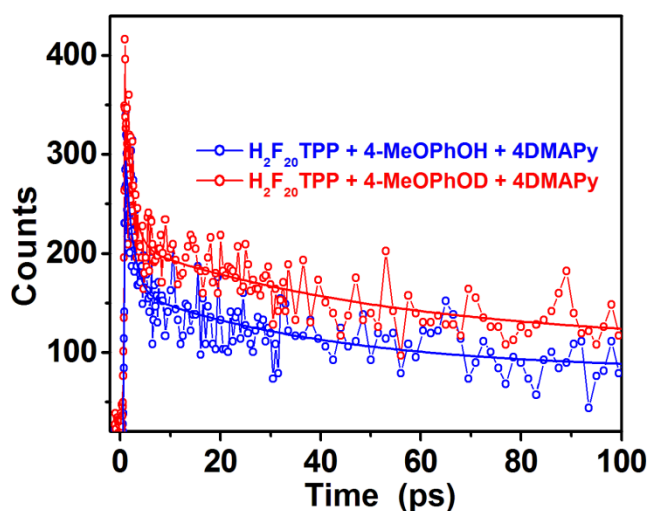


Fig.9 Fluorescence up-conversion decay profile of $H_2F_{20}TPP$ in presence of 0.5 M 4-MeOPhOH/4-MeOPhOD (blue/red) and 0.5M 4DMAPy on excitation at 410 nm. Smooth solid lines are three-exponential fits of the experimental data.

the added pyridines. The translational diffusion ($\sqrt{4D_T\tau}$)²⁹ of $H_2F_{20}TPP$ in this time scale could be $< \sim 1\text{\AA}$ considering translational diffusion coefficient³⁰ (D_T) of $H_2F_{20}TPP$ to be $1.23 \times 10^{-9} \text{ m}^2\text{s}^{-1}$. Hence, the origin of this additional fast decay component can only be rationalized considering the ultrafast electron transfer from hydrogen bonded phenol base pair to singlet excited $H_2F_{20}TPP$. The quenching rate constant corresponding to this decay ($k_{QB}^{fast} = 1/\tau_{QB}^{fast}$) is above $2 \times 10^{10} \text{ s}^{-1}$ and it is in non-diffusive regime. A substantial deuterium isotope effect is also observed in this time window. Upon replacement of OH of 4-MeOPhOH by OD this decay component is found to be of 65 ± 15 ps for 4-MeOPhOD and 4DMAPy system.

Table.2 Fluorescence Up-Conversion kinetic parameters of $H_2F_{20}TPP$ in absence and in presence of phenol-base pairs upon excitation at 410nm.

Phenol	Base	τ_1 (ps)	$a_1(\%)$	$\tau_2(\text{ps})$	$a_2(\%)$	$\tau_3(\text{ns})$	$a_3(\%)$
----	----	2 ± 0.5	~ 15	100 ± 10	$\sim -50^b$	> 9	~ 85
	Py	1.6 ± 0.5	~ 32	60 ± 10^c	$\sim 40^e$	> 3	~ 28
4-MeOPhOH	DMPy	1.6 ± 0.5	~ 46	48 ± 10^c	$\sim 32^e$	> 3	~ 21
	TMPy	1.6 ± 0.5	~ 30	45 ± 7^c	$\sim 16^e$	> 3	~ 54
	4DMAPy	1.6 ± 0.5	~ 48	40 ± 10^c	$\sim 30^e$	> 1.5	~ 27
4-MeOPhOD ^d	4DMAPy	1.6 ± 0.5	~ 50	60 ± 10^c	25^e	> 2	~ 25
	2,6-DiMeOPhOH	1.6 ± 0.5	~ 33	200 ± 10^f	$\sim 66^f$	-	-

a_1, a_2, a_3 are amplitude of respective components, ^b negative amplitude indicates that the respective component is a rise instead of decay, ^c decay time of newly appear fast component in presence of phenol and base (fast τ_{QB}), ^d Isotope effect, ^e amplitude of newly appear fast component in presence of phenol and base (a_{QB}), ^f decay time and amplitude of diffusive PCET respectively.

This result confirms that appearance of additional fast decay component is due to ultrafast PCET reaction. However, fluorescence up-conversion experiment was carried out for Case-II with 2,6-DiMeOPhOH (0.02-2M) as function different concentration for all the studied bases but no ultrafast PCET reaction was observed. In all cases two components decay were observed. A very fast 2 ps intrinsic decay of $H_2F_{20}TPP$ and a slow component decay which is broadly in agreement with the value observed in TCSPC measurement (Fig S8, ESI[†]). Hence, in this case of 2,6-DiMeOPhOH and base pair ultrafast PCET reaction does not occur. It is important to note here that hydrogen bonding interaction between 2,6-DiMeOPhOH and different bases are relatively weak to that of 4-MeOPhOH and steric effect may play the role to control the formation of hydrogen bonding equilibrium between 2,6-DiMeOPhOH and bases due to the presence of two methoxy groups on both sides of OH group hindering the ultrafast PCET reaction to occur. However, described results reveal that, the time scale of proton movement in case of non-diffusive PCET reaction is $\sim 40-60$ ps for these studied systems. To unveil the complete mechanism of this first ever seen non-diffusive PCET reaction, ultrafast transient absorption spectroscopic studies are planned soon.

4. Conclusions

In conclusion, we are able to delineate the reductive fluorescence quenching of free base porphyrin $H_2F_{20}TPP$ in DCM solvent by steady state and time resolved spectroscopic methods from picosecond to nanosecond time regime. The enhanced quenching process involves electron transfer from phenol-pyridine base pair to excited singlet state of porphyrin with concerted motion of bound proton to associated pyridine. This reaction occurs both in non-diffusive (ultrafast PCET) and diffusive regimes for 4-MeOPhOH while it restricts to diffusive regime for 2,6-DiMeOPhOH. These results may aid in understanding the PCET reaction involved in various biological processes in ultrafast time

scale.

Acknowledgements

PRB acknowledge the support from Department of Science and Technology, Government of India, Grand No. SR/S1/PC-59/2009
 Authors extends their sincere thanks to Dr. V. J. Rao for his constant encouragement and support to install femtosecond laser setup at CSIR-IICT.

References

- (a) R. A. Marcus and N. Sutin, *Biochimica et Biophysica Acta (BBA) - Reviews on Bioenergetics*, 1985, **811**, 265; R. A. Marcus, *Annu. Rev. Phys. Chem.*, 1964, **15**, 155; (b) M. R. Wasielewski, *Chem. Rev.*, 1992, **92**, 435; V. Balzani, *Electron transfer in chemistry*, Wiley-VCH, Weinheim, New York, 2001; G. J. Kavarnos and N. J. Turro, *Chem. Rev.*, 1986, **86**, 401; G. J. Kavarnos, *Fundamentals of photoinduced electron transfer*; VCH Publishers, 1993.
- A. Muller, H. Ratajczak, W. Junge and E. Diemann, *Electron and Proton Transfer in Chemistry and Biology, Studies in Physical and Theoretical Chemistry*, Elsevier, Amsterdam, 1992, vol. 78.
- (a) R. I. Cukier and D. G. Nocera, *Annu. Rev. Phys. Chem.*, 1998, **49**, 337; (b) J. M. Mayer, *Annu. Rev. Phys. Chem.*, 2004, **55**, 363; (c) M. H. V. Huynh and T. J. Meyer, *Chem. Rev.*, 2007, **107**, 5004; (d) E. A. Leo, R. Tormos and M. A. Miranda, *Chem. Commun.*, 2005, **41**, 1203; (e) E. R. Young, J. Rosenthal and D. G. Nocera, *Chem. Commun.*, 2008, **44**, 2322; (f) J. C. Freys, G. Bernardinelli and O. S. Wenger, *Chem. Commun.*, 2008, **44**, 4267; (g) L. Hammarström and S. Styring, *Energy. Environ. Sci.*, 2011, **4**, 2379.
- (a) S. H. Schiffer, *Acc. Chem. Res.*, 2001, **34**, 273; (b) S. H. Schiffer, *Chemphyschem*, 2002, **3**, 33; (c) S. H. Schiffer, *Acc. Chem. Res.*, 2009, **42**, 1881; (d) S. H. Schiffer, *Chem. Rev.*, 2010, **110**, 6937.
- (a) R. J. Debusk, B. A. Barry, I. Sithole, G. T. Babcock, L. McIntosh, *Biochemistry*, 1988, **27**, 9071; (b) Y. Z. Hu, S. Tsukiji, S. Shinkai, S. Oishi, I. Hamachi, *J. Am. Chem. Soc.*, 1999, **122**, 241; (c) H. Kurreck, M. Huber, *Angew. Chem. Int. Ed.*, 1995, **34**, 849; (d) J. L. Sessler, B. Wang, A. Harriman, *J. Am. Chem. Soc.*, 1995, **117**, 704; (e) A. Harriman, D. J. Magda and J. L. Sessler, *J. Phys. Chem.*, 1991, **95**, 1530;
- (a) L. Biczok, N. Gupta and H. Linschitz, *J. Am. Chem. Soc.*, 1997, **119**, 12601; (b) N. Gupta and H. Linschitz, *J. Am. Chem. Soc.*, 1997, **119**, 6384.
- (a) A. Magnuson, H. Berglund, P. Korall, L. Hammarström, B. Akermark, S. Styring and L. Sun, *J. Am. Chem. Soc.*, 1997, **119**, 10720; (b) M. Sjodin, S. Styring, B. Akermark, L. Sun and L. Hammarström, *J. Am. Chem. Soc.*, 2000, **122**, 3932; (c) M. Sjodin, S. Styring, H. Wolpher, Y. Xu, L. Sun and L. Hammarström, *J. Am. Chem. Soc.*, 2005, **127**, 3855; (d) M. Sjodin, R. Ghanem, T. Polivka, J. Pan, S. Styring, L. Sun, V. Sundstrom and L. Hammarstrom, *Phys. Chem. Chem. Phys.*, 2004, **6**, 4851.
- S. Y. Reece and D. G. Nocera, *J. Am. Chem. Soc.*, 2005, **127**, 9448.
- (a) D. Shukla, R. H. Young and S. Farid, *J. Phys. Chem. A*, 2004, **108**, 10386; (b) C. Turro, C. K. Chang, G. E. Leroi, R. I. Cukier and D. G. Nocera, *J. Am. Chem. Soc.*, 1992, **114**, 4013; (c) M. C. Y. Chang, C. S. Yee, D. G. Nocera and J. Stubbe, *J. Am. Chem. Soc.*, 2004, **126**, 16702; (d) M. W. Lehmann and D. H. Evans, *J. Phys. Chem. B*, 2001, **105**, 8877; (e) J. M. Mayer, D. Hrovat, J. L. Thomas and W. T. Borden, *J. Am. Chem. Soc.*, 2002, **124**, 11142; (f) J. M. Anglada, *J. Am. Chem. Soc.*, 2004, **126**, 9809; (g) S. C. Weatherly, I. V. Yang, P. A. Armistead and H. H. Thorp, *J. Phys. Chem. B*, 2003, **107**, 372; (h) J. Stubbe, D. G. Nocera, C. S. Yee and M. C. Y. Chang, *Chem. Rev.*, 2003, **103**, 2167; (i) G. A. DiLabio and K. U. Ingold, *J. Am. Chem. Soc.*, 2005, **127**, 6693; (j) M. H. V. Huynh and T. J. Meyer, *Proc. Natl. Acad. Sci. U.S.A.*, 2004, **101**, 13138; (k) T. J. Meyer and M. H. V. Huynh, *Inorg. Chem.*, 2003, **42**, 8140.
- (a) T. Kojima, T. Sakamoto, Y. Matsuda, K. Ohkubo and S. Fukuzumi, *Angew. Chem. Int. Ed.*, 2003, **42**, 4951; (b) R. M. Haddox, H. O. Finklea, *J. Electroanal. Chem.*, 2003, **351**, 550.
- (a) J. K. Kochi, *Free Radicals*; Ed, Wiley, New York, 1973; (b) J. M. Mayer, *Acc. Chem. Res.*, 1998, **31**, 441.
- (a) S. Prashanthi and P. R. Bangal, *Chem. Commun.*, 2009, **45**, 1757; (b) P. H. Kumar, S. Prashanthi and P. R. Bangal, *J. Phys. Chem. A*, 2011, **115**, 631.
- (a) J. Rosenthal, J. M. Hodgkiss, E. R. Young, and D. G. Nocera, *J. Am. Chem. Soc.*, 2006, **128**, 10474; (b) N. H. Damrauer, J. M. Hodgkiss, J. Rosenthal, and D. G. Nocera, *J. Phys. Chem. B*, 2004, **108**, 6315.
- Dolphin D (ed), *The Porphyrins*, Vols. I–VII. Academic, New York.
- (a) M. R. Wasielewski, *Chem. Rev.*, 1992, **92**, 435; (b) M. D. Ward, *Chem. Soc. Rev.*, 1997, **26**, 365.
- G. McDermott, S. M. Prince, A. A. Freer, A. M. Hawthornthwaite-Lawless, M. Z. Papiz, R. J. Cogdell and N. W. Isaacs, *Nature*, 1995, **374**, 517.
- R. A. Huber, *Angew. Chem. Int. Ed. Engl.*, 1989, **28**, 848.
- (a) M. R. Shortreed, S. F. Swallen, Z. Y. Shi, W. Tan, Z. Xu, C. Devadoss, S. Moore and R. J. Kopelman, *J. Phys. Chem. B*, 1997, **101**, 6318; (b) J. Seth, V. Palaniappan, T. E. Johnson, S. Prathapan, J. S. Lindsey and D. F. Bocian, *J. Am. Chem. Soc.*, 1994, **116**, 10578; (c) F. R. Li, S. I. Yang, Y. Z. Ciringh, J. Seth, C. H. Martin, D. L. Singh, D. H. Kim, R. R. Birge, D. F. Bocian, D. Holten and J. S. Lindsey, *J. Am. Chem. Soc.*, 1998, **120**, 10001.
- S. Prashanthi, P. H. Kumar, L. Wang, A. K. Perepogu and P. R. Bangal, *J. Fluoresc.*, 2010, **20**, 571.
- N. Mataga and S. Tsuno, *Bull. Chem. Soc. Jpn.*, 1957, **30**, 368.
- A. M. Dierckx, P. Huyskens and H. Zeegers, *J. Chim. Phys.*, 1965, **62**, 336.
- P. R. Bangal, *Chem. Phys. Lett.*, 2005, **401**, 200.
- D. Rehm and A. Weller, *Isr. J. Chem.*, 1970, **8**, 259.
- Berces and H. Linschitz, *J. Am. Chem. Soc.*, 1997, **119**, 11071.
- J. A. Hodge, M. G. Hill and H. B. Gray, *Inorg. Chem.*, 1995, **34**, 809.
- S. Carrigan, S. Doucette, C. Jones, C. J. Marzocco and M. A. Halpern, *J. Photochem. Photobiol. A*, 1996, **99**, 29.
- S. C. Weatherly, I. V. Yang and H. H. Thorp, *J. Am. Chem. Soc.*, 2001, **123**, 1236; V. Shafirovich, A. Dourandin and N. E. Geacintov, *J. Phys. Chem. B*, 2001, **105**, 8431; V. Shafirovich, S. H. Courtney, N. Ya and N. E. Geacintov, *J. Am. Chem. Soc.*, 1995, **117**, 4920.
- J. S. Baskin, H. Z. Yu and A. H. Zewail, *J. Phys. Chem. A*, 2002, **106**, 9837.
- J. R. Lakowicz, *Principle of fluorescence spectroscopy*, 3rd ed, Springer, New York, 2006.
- H. Saiki, K. Takami and T. Tominaga, *Phys. Chem. Chem. Phys.*, 1999, **1**, 303.

Ultrafast Photo-induced Proton Coupled Electron Transfer is observed for the first time from H-bonded phenols to Pentafluorophenyl Porphyrin indicating proton movement time to be 40-60 ps depending on the base used.

